

Native defect related optical properties of ZnGeP₂

N. Dietz

Department of Materials Science and Engineering, North Carolina State University, Raleigh, North Carolina 27695

I. Tsveybak and W. Ruderman

Inrad, Inc., Northvale, New Jersey 07647

NASA-CR-202489

G. Wood and K. J. Bachmann

Department of Materials Science and Engineering, North Carolina State University, Raleigh, North Carolina 27695

(Received 14 July 1994; accepted for publication 26 September 1994)

We present photoluminescence, photoconductivity, and optical absorption spectra for ZnGeP₂ crystals grown from the melt by gradient freezing and from the vapor phase by high pressure physical vapor transport (HPVT). A model of donor and acceptor related subbands in the energy gap of ZnGeP₂ is introduced that explains the experimental results. The emission with peak position at 1.2 eV is attributed to residual disorder on the cation sublattice. The lower absorption upon annealing is interpreted in terms of both the reduction of the disorder on the cation sublattice and changes in the Fermi level position. The *n*-type conductivity of ZnGeP₂ crystals grown under Ge-deficient conditions by the HPVT is related to the presence of additional donor states. © 1994 American Institute of Physics.

Zinc germanium phosphide is a chalcopyrite structure semiconductor with a minimum pseudodirect band gap of ~2.1 eV at room temperature.¹ It has a relatively large second-order susceptibility tensor component ($d_{36}=75$ pm/V) and an attractive transparency range² extending from 0.67 to 13 μ m. In view of its substantial birefringence of 0.36%, ZnGeP₂ is thus suitable for phase-matched nonlinear optical applications in the infrared, e.g., the fabrication of optical parametric oscillators and harmonic generation/sum frequency mixing based on powerful infrared laser sources.³ In addition, ZnGeP₂ is of interest in the context of nearly lattice-matched heteroepitaxy of compound semiconductors on silicon.⁴

The phase relations in the ternary system Zn, Ge, P are documented on the ZnP₂-Ge pseudobinary, indicating a congruent melting point at composition ZnGeP₂.⁵ ZnGeP₂ single crystals have been grown from the melt by the gradient freezing⁵ and horizontal Bridgman methods.⁶ Recently we have reported the growth of ZnGeP₂ crystals by high pressure physical vapor transport⁷ and the heteroepitaxial organometallic chemical vapor deposition growth of ZnGeP₂ on GaP and Si substrates, respectively.⁸

ZnGeP₂ crystals grown from the melt are semi-insulating ($\rho \approx 10^6 \Omega$ cm) and exhibit *p*-type conductivity. The carrier mobility in such crystals is $10 \text{ cm}^2/\text{V s} \leq \mu_p \leq 40 \text{ cm}^2/\text{V s}$ at a net acceptor concentration of $10^{10} \text{ cm}^{-3} \leq N_A - N_D \leq 10^{12} \text{ cm}^{-3}$, suggesting a high compensation level (10^{19} cm^{-3}).⁹ ZnGeP₂ crystals grown by metalorganic chemical vapor deposition and high pressure physical vapor transport (HPVT) are low resistivity *p* type and high resistivity *n* type, respectively. In the optical absorption spectra at room temperature bands at 1.31, 1.46, 1.58, 1.67, and 1.80 eV are observed.¹⁰ Annealing of the crystals for 300 h at 500 °C was found to be effective in reducing the residual absorption in the 0.67–3 μ m region.¹¹ Polarized photoluminescence (PL) and cathodoluminescence studies revealed bands in the 1.3–

1.4 and 1.6–1.7 eV region, which were assigned to transitions between conduction bands states and a deep triplet acceptor band.¹²

PL studies extending over the visible and infrared wavelength range (500–1700 nm) reveal, independent of the method of growth, a broad emission band with peak position at 1.2 eV. The luminescence was detected with a GaInAs photomultiplier tube (PMT) and a Ge detector, being cooled with liquid nitrogen and having cutoffs at ~1.2 and 0.7 eV, respectively. This combination of detectors is essential since, due to the cutoff at 1.2 eV, the use of the PMT results in a false peak position of the infrared luminescence near 1.3 eV. Figure 1 shows typical PL spectra for (a) ZnGeP₂ platelets

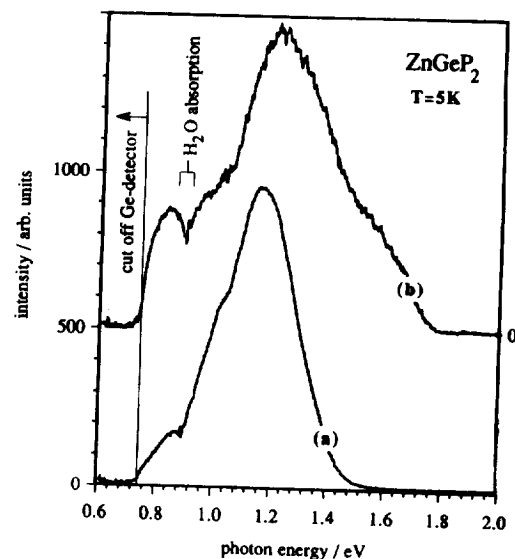


FIG. 1. PL spectra of ZnGeP₂ crystals grown by (a) high pressure vapor transport and (b) gradient freezing.

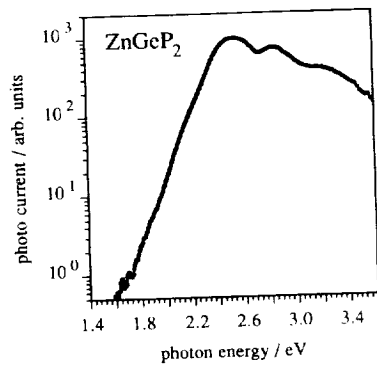


FIG. 2. Photoconductivity spectrum of bulk ZnGeP₂ crystal wafer that is cut from a crystal grown by the gradient freezing method.

grown by the HPVT method and (b) ZnGeP₂ cut from a bulk single crystal grown by the gradient freezing method. The structure near 0.9 eV is due to H₂O absorption. In the vicinity of the nucleation point, HPVT grown ZnGeP₂ crystals exhibit additional near-edge emission, which shifts toward the infrared upon continued growth. After prolonged periods of HPVT only the 1.2 eV PL remains. The PL of as-grown bulk single crystals is also dominated by 1.2 eV emission with a high energy shoulder extending to ~1.8 eV. Annealing of the crystal in vacuum at 500 °C for 400 h results in a substantial increase of the 1.7 eV emission relative to the 1.2 eV emission. In order to check as to whether or not the points defects that give rise to the higher energy emission are preferentially formed near the surface, we removed ~1 μm from the surface of the annealed crystal by etching, which caused a significant lowering of the PL near 1.7 eV.

Figure 2 shows a PC spectrum for the same bulk crystal in the as-grown state. The PC reveals subband-gap excitation extending to ~1.6 eV with three characteristic peaks at 2.5, 2.85, and 3.2 eV. Figure 3 shows the changes of the absorption coefficient in the transparency region of the same ZnGeP₂ crystal that occur in the course of the annealing at 500 °C. A significant reduction in the near-infrared absorption is observed.

Studies of the time dependence of the PL in the range 1.2–1.6 eV, which will be described in more detail in a forthcoming publication,¹³ reveal hyperbolic decay behavior. The decay time decreases toward higher energies. Upon increasing the limits on the time window, the time-resolved spectra of the broad emission band exhibit a shift of the high energy edge to lower energies. For a given time window the intensity of the high energy edge of the PL decreases with increasing temperature between 5 and 100 K.

Because of the hyperbolic decay of the PL, we interpret the steady state luminescence shown in Fig. 1 in terms of transitions between donor and acceptor states associated with energy subbands in the band gap of ZnGeP₂ that are shown in Fig. 4. The broad PL band, peaked at 1.2 eV, can be attributed to transitions between donor (D_1) and acceptor (A_1) states that are associated with subbands below the absorption edge having a center distance of 1.2 eV. Explaining the structure in the PC spectra by transitions between filled A_1 states and the conduction band edge (CBE), the highest

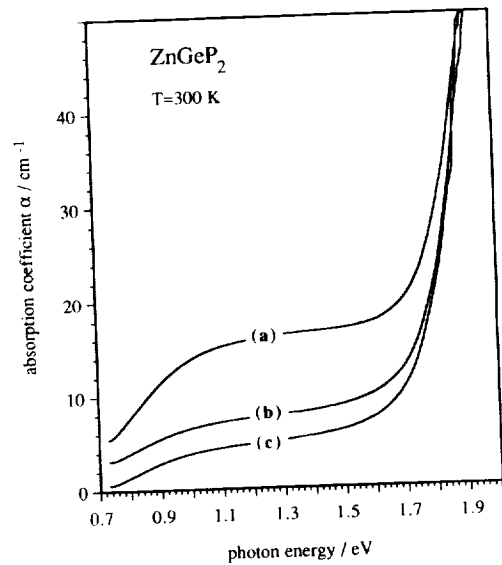


FIG. 3. Absorption spectra for as-grown and annealed crystal wafers that are cut from a ZnGeP₂ crystal grown by the gradient freezing method. (a) As grown, (b) annealed for 300 h, and (c) annealed for 400 h at 500 °C in vacuum.

filled A_1 state is associated with an energy eigenvalue of ~1.6 eV below the CBE. Since the width of the broad subband-gap luminescence is at least 1 eV, this places the lower edge of the A_1 subband close to the upper valence band edge (VBE).

Figure 5 shows a schematic representation of some of the point defects that may be generated upon deviation of the ternary compound composition from stoichiometric ZnGeP₂, e.g., Zn_□, Ge_□, and P_□ vacancies and the formation of various antisite defects. Note that specific deviations from stoichiometry within the homogeneity range about stoichiometric ZnGeP₂ merely establish the predominance of specific native point defects, but preclude neither the presence of other defects nor interactions with extrinsic point defects. Although the point defect chemistry is thus complex, hints for the predominance of certain defects are obtained by the analysis of the annealing behavior and the behavior associated with specific growth conditions. The growth tempera-

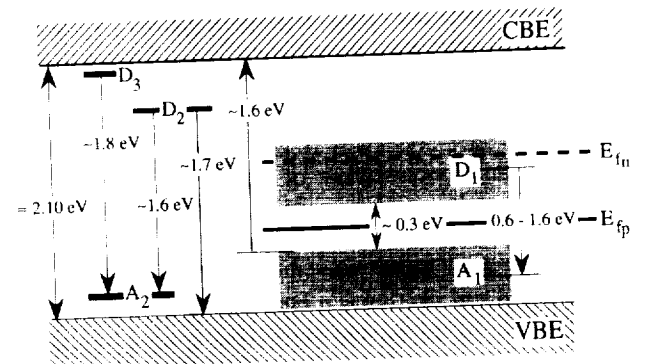


FIG. 4. Suggested model of the positions of various donor and acceptor related subbands in the band gap of ZnGeP₂. E_{fp} is the Fermi level for p -type and E_{fn} the FL position for n -type ZnGeP₂ crystals.

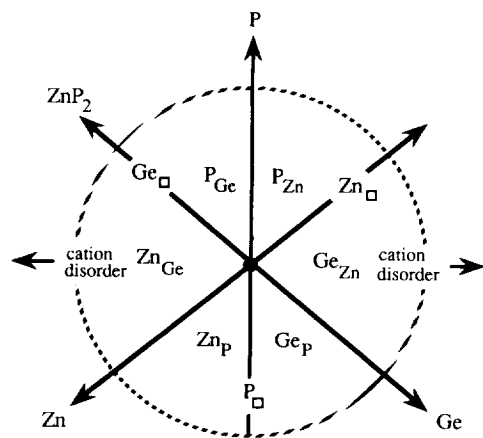


FIG. 5. Schematic representation of native point defects that may be generated upon deviations from stoichiometric in the homogeneity range of ZnGeP_2 .

ture under the conditions of GF and HPVT is above the order-disorder transformation between the chalcopyrite and zinc-blende structures of ZnGeP_2 which occurs at $\sim 950^\circ\text{C}$. Thus residual disorder that is quenched-in during cooling may persist in a metastable state at room temperature. It corresponds to the simultaneous existence of nonequilibrium populations of Ge_{Zn} and Zn_{Ge} antisite defects.

In agreement with the suggestion of Rud and Masagutova¹¹ we attribute the residual absorption in the transparency range of ZnGeP_2 to transitions from the A_1 subband into the conduction band and the D_1 donor band. From the extension of the absorption to $\sim 5 \mu\text{m}$,¹³ we can conclude that the lower edge of the D_1 band extends to ~ 0.30 eV above the upper edge of the A_1 band, placing the lowest states belonging to the D_1 subband at ~ 1.30 eV below the CBE. Thus, in the absence of other point defects, the Fermi level (FL) is pinned to a position between the A_1 and D_1 subbands in the lower half of the band gap of ZnGeP_2 , explaining the high resistivity p -type conductivity. Of course, the presence of additional donors and acceptors that are unrelated to the D_1 and A_1 subbands can contribute to the residual absorption which may be due to both additional $A-D$ transition pathways and the associated shift in the Fermi level that affects the concentrations of filled acceptor and unfilled donor states.

The transitions between filled A_1 and empty D_1 states do not contribute to the PC spectra because of the large effective mass in the D_1 subband due to the localization of the associated donor states. The above interpretation is reinforced by the time-dependent recombination behavior starting with fast high energy transitions related to $D-A$ pairs in close proximity that are followed by a slower recombination at lower energies corresponding to larger separations between the localized $D-A$ pairs.

There are at least three effects that must be considered in the interpretation of the annealing studies: (i) The reduction of quenched-in disorder, reducing the concentration of point defects, (ii) The shift of the FL position associated with this annihilation of defects, altering the population of the remain-

ing defect states, and (iii) shifts in the FL position caused by the generation of defects at the crystal surface upon annealing. The observation of additional structure at higher energy in the PL and the depth dependence of the luminescence features after annealing clearly establishes additional point defect generation due to the loss of zinc and phosphorus at the surface followed by diffusion into the subsurface region. Consequently the luminescence near 1.6 and 1.7 eV are attributed to transitions between donor states D_2 (e.g., P_\square) and acceptor states A_2 (e.g., Ge_p) or VBE, respectively.

A more definitive control of the stoichiometry of ZnGeP_2 is obtained by growth from the vapor phase. Thermochemical calculations of the temperature dependence of the existence range of ZnGeP_2 show that HPVT of ZnGeP_2 from a molten source initiates at substantial Zn supersaturation, that is, the vapor composition determined by the partial pressures over a source of molten ZnGeP_2 ties at the lower substrate temperature into Ge-deficient compositions within the homogeneity range about ZnGeP_2 . For stationary sources, Zn depletion ensues during the course of the HPVT experiment, resulting in the later stages of growth in a conversion from Ge-deficient to Zn-deficient growth conditions. The n -type conductivity of ZnGeP_2 crystals grown by the HPVT method from an undepleted source composition suggests the formation of relatively shallow donor states D_3 (e.g., P_{Ge}) that move the FL toward the CBE. The high infrared transparency of the crystals reported by Xing *et al.*⁷ is thus explained as a combined effect of the elimination of Ge_{Zn} sites and FL motion that results in the filling of residual deep Ge_{Zn} donor states by electrons. The near-edge PL observed shortly after the nucleation of ZnGeP_2 crystals under the conditions of HPVT can be associated with $D-A$ transitions involving P_{Ge} donor states and Ge_\square , Zn_\square , or Zn_{Ge} acceptor states. The conversion to exclusively 1.2 eV emission for HPVT crystals after prolonged periods of growth is consistent with the gradual replacement of P_{Ge} by Ge_{Zn} antisite defects upon conversion from Ge- to Zn-deficient growth conditions.

This work has been supported by NSF Grants DMR 9202210 and SBIR No. III-9316988 and NASA Grants NAGW-2865 and NAS 1-19586.

¹J. L. Shay and J. H. Wernick, *Ternary Chalcopyrite Structure Semiconductors* (Academic, New York, 1976).

²G. D. Boyd, H. M. Kasper, J. H. McFee, and F. G. Storz, *IEEE J. Quantum Electron.* **QE-8**, 900 (1972).

³Y. M. Andreev, V. G. Voevodin, A. I. Gribenyukov, and V. P. Novikov, *Sov. J. Quantum Electron.* **17**, 748 (1987).

⁴K. J. Bachmann, *Mater. Res. Soc. Symp. Proc.* **242**, 707 (1992).

⁵E. Buchler, J. H. Wernick, and J. D. Wiley, *J. Electron. Mater.* **2**, 796 (1973).

⁶A. L. Gentile and O. M. Stafsud, *Mater. Res. Bull.* **9**, 105 (1974).

⁷G. C. Xing and K. J. Bachmann, *Appl. Phys. Lett.* **56**, 271 (1990).

⁸G. C. Xing, K. J. Bachmann, J. B. Posthill, and M. L. Timmons, *J. Appl. Phys.* **69**, 4286 (1991).

⁹A. Sodeika, A. Z. Silevicius, Z. Januskevicius, and A. Sakalas, *Phys. Status Solidi A* **69**, 491 (1982).

¹⁰I. S. Gorban, V. V. Grishchuk, and I. G. Tregub, *Sov. Phys. Semicond.* **18**, 567 (1984).

¹¹Y. V. Rud and R. V. Masagutova, *Sov. Tech. Phys. Lett.* **7**, 72 (1981).

¹²J. E. McCrae, Jr., M. R. Gregg, R. L. Hengehold, Y. K. Yeo, P. H. Ost典iek, M. C. Ohmer, P. G. Schunemann, and T. M. Pollak, *Appl. Phys. Lett.* **23**, 3142 (1994).

¹³N. Dietz, W. Busse, H. E. Gumlich, W. Rüdeman, I. Tsveybak, G. Wood, and K. J. Bachmann (unpublished results, 1994).

